

Flexible Zn-MOF Exhibiting Selective CO₂ Adsorption and Efficient Lewis Acidic Catalytic Activity

Rashmi A. Agarwal, Anoop K. Gupta, and Dinesh De

Cryst. Growth Des., **Just Accepted Manuscript** • DOI: 10.1021/acs.cgd.8b01462 • Publication Date (Web): 12 Feb 2019

Downloaded from <http://pubs.acs.org> on February 12, 2019

Just Accepted

“Just Accepted” manuscripts have been peer-reviewed and accepted for publication. They are posted online prior to technical editing, formatting for publication and author proofing. The American Chemical Society provides “Just Accepted” as a service to the research community to expedite the dissemination of scientific material as soon as possible after acceptance. “Just Accepted” manuscripts appear in full in PDF format accompanied by an HTML abstract. “Just Accepted” manuscripts have been fully peer reviewed, but should not be considered the official version of record. They are citable by the Digital Object Identifier (DOI®). “Just Accepted” is an optional service offered to authors. Therefore, the “Just Accepted” Web site may not include all articles that will be published in the journal. After a manuscript is technically edited and formatted, it will be removed from the “Just Accepted” Web site and published as an ASAP article. Note that technical editing may introduce minor changes to the manuscript text and/or graphics which could affect content, and all legal disclaimers and ethical guidelines that apply to the journal pertain. ACS cannot be held responsible for errors or consequences arising from the use of information contained in these “Just Accepted” manuscripts.



Flexible Zn-MOF Exhibiting Selective CO₂ Adsorption and Efficient Lewis Acidic Catalytic Activity

Rashmi A. Agarwal,^{a*} Anoop K. Gupta,^b Dinesh De^b

^aDepartment of Civil Engineering, Indian Institute of Technology Kanpur, Kanpur 208016, India

^bDepartment of Chemistry, Indian Institute of Technology Kanpur, Kanpur 208016, India

ABSTRACT: A two dimensional, tetragonal porous metal organic framework $\{[\text{Zn}_2(\text{TBIB})_2(\text{HTCPB})_2]\cdot 9\text{DMF}\cdot 19\text{H}_2\text{O}\}_n$ (**1**) has been synthesized under hydrothermal conditions by employing 1,3,5-tri(1H-benzo[d]imidazol-1-yl)benzene (TBIB) and 1,3,5-Tris(4'-carboxyphenyl-)benzene (H₃TCPB). But non-covalent supramolecular interactions between the layers make this framework three dimensional, generating porosity in one dimension. Flexibility arises due to the presence of two types of large linkers wherein some functional groups of the ligands are not coordinated with the metal ion. Desolvated polymer shows moderate CO₂ uptake (65 cm³ g⁻¹ at 195 K and 1 bar) at low temperature and pressure. Compound **1** acts as a highly efficient heterogeneous catalyst towards the formation of cyclic carbonate through cycloaddition of CO₂ as well as towards the synthesis of quinoline derivatives by the Friedländer reaction. Presence of the free -COOH, -C=O groups and uncoordinated -N atoms on the wall of the pores make this framework an excellent candidate for the catalytic reactions without activation of the compound.

INTRODUCTION

The field of porous coordination polymers (PCPs) or metal organic frameworks have attracted a tremendous attention due to their large surface area, tuneable pore sizes and versatile architectures, lead to a variety of applications such as gas adsorption, separation and heterogeneous catalysis.¹⁻¹⁰ PCPs are often much more dynamic and flexible (3rd generation

1
2
3 compounds) which is due to the supramolecular non-bonding interactions present within the
4 framework. Utilization of two large linkers causes flexibility in the framework due to
5
6 adjustment of the linkers according to the coordination modes of the metal ion. In the
7
8 presence or absence of guest molecules adjustments take place within the framework
9
10 according to the availability of the space due to the presence of different types of non-
11
12 bonding interactions shown by shrinking or elongation of the framework.¹¹ These structures
13
14 can be transformed depending upon the external stimuli and thus having unique properties.
15
16 Specifically ligand molecules undergo rotation due to the presence of large space.¹²
17
18

19
20 Exertion of abundantly available CO₂ towards the synthesis of fine chemicals is a recently
21
22 very sustainable approach.^{13,14} Global warming due to the high release of CO₂ from
23
24 anthropogenic activities have attracted huge global drive towards the carbon dioxide capture
25
26 and sequestration.¹⁵
27
28

29
30 Most of the previous studies have shown that formation of cyclic carbonate and other
31
32 catalytic reactions occur due to presence of open metal sites.¹⁶ MOF functionalized with
33
34 nitrogen bases and other polar functional groups (-NH₂, -OH, -NO₂, -COOH, -SO₃H, etc.)
35
36 enhances the selectivity towards CO₂.¹⁷
37
38

39
40 In the MOFs, vacant metal sites are generated by removing the metal bound solvent
41
42 molecules. This process needs too much time, because first solvent exchange experiment is
43
44 performed to replace the lattice as well as metal bound solvent molecules by low boiling
45
46 solvent then finally, solvent exchanged sample is applied towards heating under high
47
48 vacuum. During these processes, different MOFs can lose their crystallinity as well as, the
49
50 chances for collapsing the frameworks are increases.¹⁸ But recent studies have shown that
51
52 host guest interactions are very important for high gas uptake as well for excellent catalytic
53
54 activity.¹⁹
55
56
57
58
59
60

1
2
3 Herein the synthesized MOF have a number of free functional groups (-COOH, C=O and -N)
4 which efficiently catalyse the reaction without activating the compound. Effective means for
5 addressing environmental issues, the development of sustainable chemical sciences involves
6 new technologies and efficient processes. Weaker non-covalent interactions such as hydrogen
7 bonds, van der Waals forces and π - π contacts may also strongly influence the formation of
8 coordination polymers.²⁰
9
10
11
12
13
14
15
16
17

18 **EXPERIMENTAL SECTION**

19
20 **Materials and Physical Measurements.** All the chemicals were reagent grade from Aldrich
21 and used without further purification. Solvents were purchased from S. D. Fine Chemicals,
22 India. Characteristic spectroscopic techniques and X-ray structural studies have been
23 provided in the Supporting Information.
24
25
26
27
28

29 **Synthesis of 1,3,5-tri(1H-benzo[d]imidazol-1-yl)benzene (TBIB).** TBIB was synthesized
30 according to the previous study.²¹
31
32
33

34 **Synthesis of 1,3,5-Tris(4'-carboxyphenyl)-benzene (H₃BTB).** H₃BTB was prepared
35 according to the published procedure.²²
36
37
38

39 **Synthesis of {[Zn₂(TBIB)₂(HBTB)₂]·9DMF·19H₂O}_n.** A mixture of Zn(NO₃)₂·6H₂O (60
40 mg, 0.188 mmol), TBIB (20 mg, 0.047 mmol), H₃BTB (20.6 mg, 0.047 mmol) and
41 DMF:H₂O (3 ml, 3:1 v/v) was placed in a Teflon-lined stainless steel autoclave. The
42 autoclave was heated up to 80 °C under autogenous pressure for 48 h and then allowed to
43 cool to room temperature at a rate of 10 °C/h. Colourless crystals of the complex were
44 obtained by filtration and washed with DMF followed by acetone. Yield = 80%. Anal. Calcd.
45 for C₁₃₅H₁₇₀N₂₁O₄₀Zn₂ = C, 56.71; H, 5.95; N, 10.29%. Found: C, 56.45; H, 5.7; N, 10.40%.
46 FT-IR (KBr pellets, cm⁻¹): 3362 (broad), 1711 (m), 1672 (s), 1607 (s), 1551 (s), 1501(s),
47 1382 (s), 1231 (s), 773 (s) (Figure S1).
48
49
50
51
52
53
54
55
56
57
58
59
60

General Procedure for the Cycloaddition of CO₂ to Epoxides. As-synthesized compound (heterogeneous catalyst) was used directly without activation. Reactions were carried out in a Schlenk tube with stirring at room temperature depending on the substrate, and CO₂ (99.999%) bubbling. Epoxide (20 mmol), catalyst **1** (10 wt%), and co-catalyst TBAB (1 mmol) were added. Upon completion the reaction, the reaction mixture and catalyst were separated by filtration to obtain a crude compound. This crude mixture was given for ¹H NMR (in CDCl₃) to calculate the yield.

General Procedure for the Friedlander reaction

The reaction mixture containing 2-aminoaryl ketones (0.5 mmol), ethyl acetoacetate (1 mmol), and catalyst **1** (5 wt%) was placed in a RB at 85 °C for 24 h with continuous stirring. As confirmed by the TLC, after completion of the reaction the reaction mixture is filtered to get the crude product. This crude product was purified by column chromatography by utilizing ethyl acetate/hexane (1/10 : v/v) as eluent to get the pure product.

RESULTS AND DISCUSSION

A flexible, layered PCP has been synthesized by the hydrothermal reaction of Zn(NO₃)₂·6H₂O with TBIB and H₃TCPB in DMF and water at 80 °C for 48 h. 3D structure was generated via non-covalent supramolecular interactions between the layers creating porous structure showing 1D channels. Single crystal X-ray study reveals that **1** crystallizes in the monoclinic space group *P*2₁/*c* and asymmetric unit consisting of two Zn(II) ions, two TBIB, two HTPCB²⁻ ligands along with 9 DMF and 19 H₂O solvent molecules in the lattice. Zn1 has tetrahedral geometry MN₂O₂ with coordination from two N atoms of benzimidazole of two different TBIB and two O atoms of two carboxylates of two HTPCB²⁻ ligands (Figure 1a). Metal ions in a 1D chain are connected by TBIB ligand and layered structure is created by metal ion coordination with HTPCB²⁻ (Figure 1b). One benzimidazole -N atom of each TBIB ligand and two C=O group along with one -COOH of each HTPCB²⁻ are free. Layers

are stacked in ABAB... fashion (Figure 1c) and are connected via non-covalent hydrogen and pi-pi bonding interactions as shown in Figure 1d leading to a three dimensional porous structure with 1D channels (including Vander Wal radii $13.5 \times 8.3 \text{ \AA}^2$) along the crystallographic a axis. Solvent accessible void volume was calculated to be 38% after squeezing solvent molecules. Topological analysis was carried out by using TOPOS software showing that Zn(II) metal ion has 4 connected node with point symbol $\{4^4.6^2\}$ and topological type sql/Shubnikov tetragonal plane net (topos&RCSR.ttd) (Figure S2).

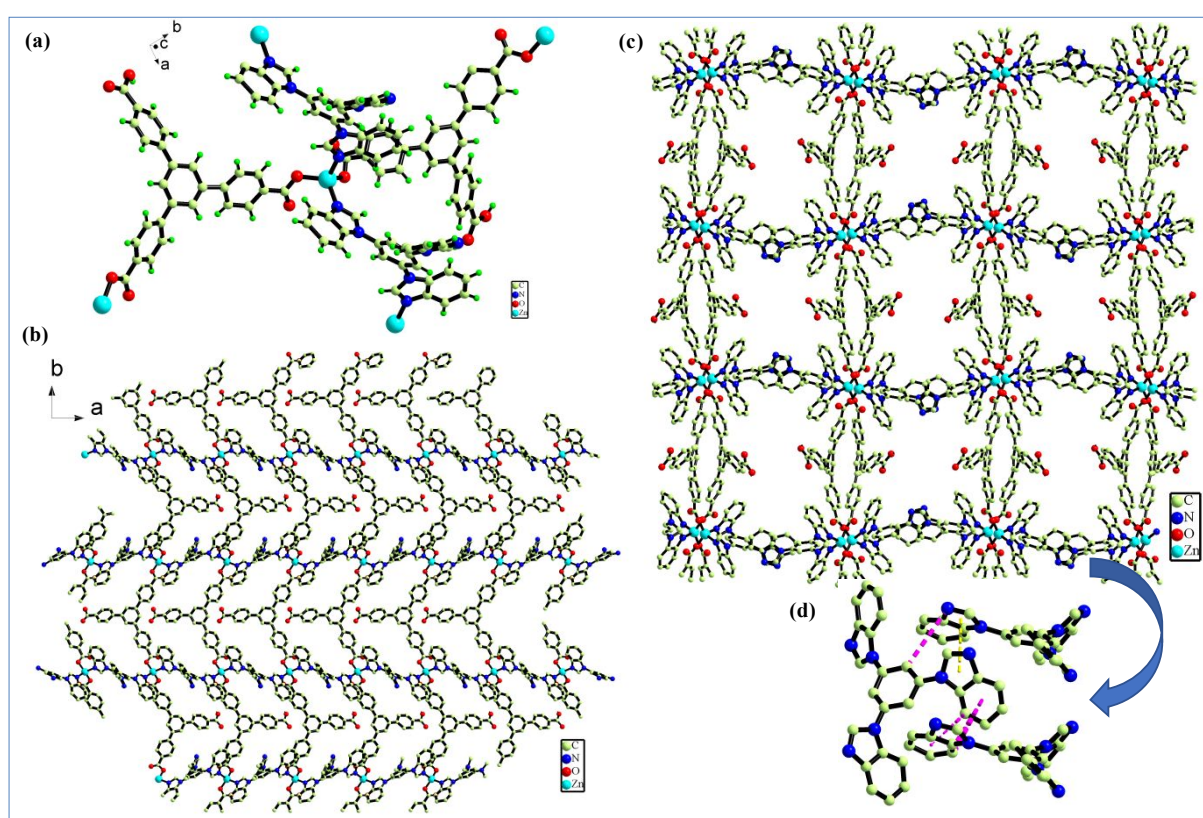


Figure 1. (a) Coordination environment around Zn(II) metal center, (b) layered structure of the polymer, (c) 3D structure and 1D pore formation through supramolecular interactions between layers, (d) interactions between TBIB of two different layers.

Thermal stability of the compound **1** has been checked by thermogravimetric analysis. TGA curve (Figure S3) shows weight loss of ~36.3% (calculated ~35%) corresponding to loss of all solvent molecules (water and DMF) from the cavities of the polymer between the

1
2
3 temperatures 80–290 °C. Compound is stable up to 350 °C after that decomposition takes
4
5 place.

6
7
8 VTPXRD measurements (Figure S4) show that compound breathe at room temperature
9
10 because in the PXRD of as-synthesized compound, diffraction peaks are slightly shifted
11
12 towards higher 2θ value when compared with the simulated pattern. It shows that framework
13
14 is slightly shrunk as temperature is increased.
15
16
17
18

19 **Gas adsorption studies**

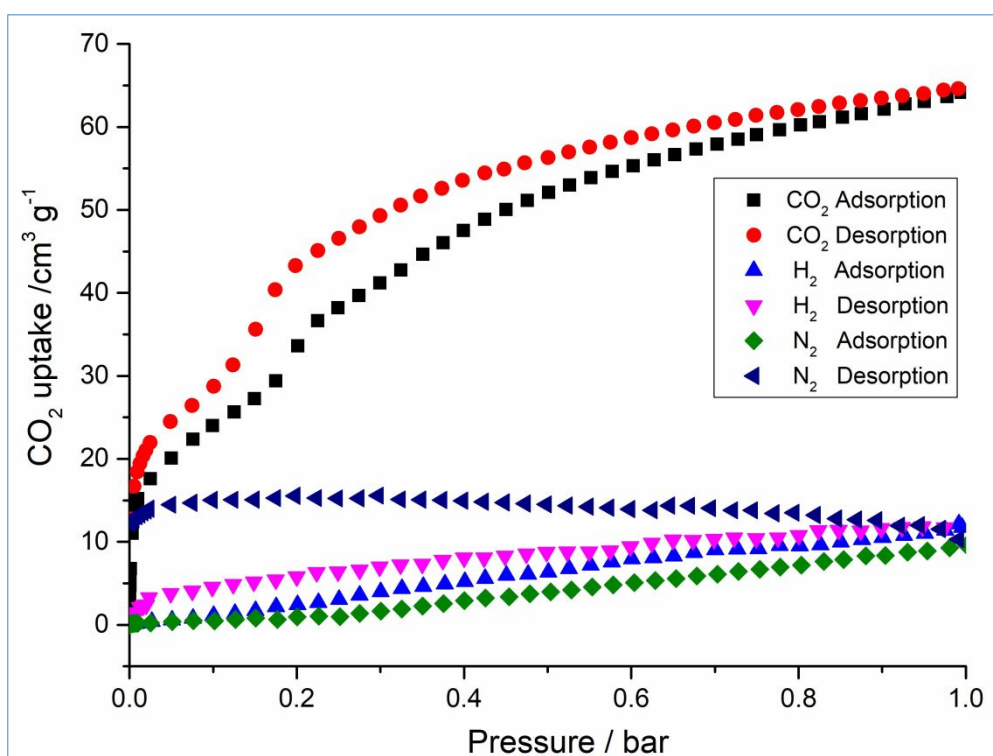
20
21
22 Before gas adsorption measurements as-synthesized compound was first activated by
23
24 immersing it in the DCM solvent to replace all the solvent molecules with the low boiling
25
26 solvent molecules. After that it was heated up to 70 °C at high vacuum to make it free from
27
28 all DCM molecules to generate **1a** (de-solvated).
29

30
31 To check the porosity of de-solvated compound **1a** gas adsorption studies have been done at
32
33 low pressure (1 bar) and low temperature for H₂ and N₂ (77 K) and for CO₂ (195 K).
34
35 Compound exhibits selectivity towards CO₂ gas showing type 1 adsorption isotherm
36
37 revealing its microporous nature with saturation adsorption up to 65 cm³g⁻¹ with slight
38
39 hysteresis at low temperature and pressure as shown in Figure 2. The Brunauer-Emmett-
40
41 Teller (BET) surface area, calculated from CO₂ sorption at 195 K is 138 m² g⁻¹. As PXRD
42
43 measurements (Figure S4) reveal that **1** is a highly flexible coordination polymer because
44
45 even at room temperature, its peaks get shifted slightly towards higher 2θ angle but at
46
47 increasing temperatures peaks shifting is more towards higher 2θ angle. It leads to the higher
48
49 shrinkage in the polymer with respect to the increase in temperature. That is why at room
50
51 temperature CO₂ adsorption is only 11.4 cm³g⁻¹ due to contraction in the framework (Figure
52
53 S6). Pore size distribution analysis shows (Figure S5) that pores have an average diameter of
54
55 1.8 nm with pore volume approximately ~0.10 cm³g⁻¹ due to shrinkage. H₂ gas is not
56
57
58
59
60

1
2
3 adsorbed due to its non-polar nature while framework has polarity due to the presence of free
4
5 functional groups in both the linkers. N₂ sorption does not takes place at the surface of the
6
7 flexible polymer due to the presence of 1D pores and large kinetic diameter of N₂. While CO₂
8
9 is a polar molecule and it needs polar environment to get inside the structure due to having
10
11 higher quadrupole moment. Presence of free -COOH, C=O groups and uncoordinated
12
13 benzimidazole N atoms provide polarity to the wall of the pore, facilitating CO₂ gas
14
15 adsorption. But in this MOF there are free carboxylic acid groups which are present at the
16
17 pore surface and CO₂ groups are also acidic in nature so gas adsorption is decreased due to
18
19 repulsive nature of the same charges.
20
21
22

23
24 Previous literature studies show that mesoporous silica materials have larger sorption
25
26 properties for CO₂ over a wide range of pressures at different temperatures reported by Sayari
27
28 et al.²³ But modified mesoporous silica structures with triamine and polyethylenimine (PEI)
29
30 functionalization with different pore lengths show fast CO₂ adsorption properties.^{24,25} CO₂
31
32 adsorption in Na-A zeolite at 273–333 K temperature and desorption at higher temperature
33
34 (573–673 K) has been reported by Zukal et. al. where small portion of CO₂ retain in the form
35
36 of surface carbonates.²⁶ Zeolitic structures cannot be functionalized/tuned according to the
37
38 requirement. High CO₂ uptake (5.28 mmol/g) have been observed in Mg-MOF-74 (CPO-27-
39
40 Mg) at 40 °C and at low pressure under dry conditions due to the strong interaction of open
41
42 metal sites (OMSs) with CO₂ molecules. But presence of moisture affects the gas uptake
43
44 because then water molecules are coordinated with the OMSs.²⁷⁻²⁹ Cu-BTC also have
45
46 unsaturated Cu metal sites which helps in CO₂ adsorption accurately calculated by employing
47
48 a combined DFT-ab initio computational scheme.³⁰ Synthesis of functionalized MOFs by
49
50 introducing a high density of free amine groups in Mg-MOF-74 showed exceptionally high
51
52 uptake of CO₂ due to strong affinity towards CO₂ even in the presence of high humidity.³¹
53
54
55
56
57
58
59
60

1
2
3 Monodentate hydroxide also have strong reversible interaction with CO₂ via the formation
4 and decomposition of bicarbonate.³² But in present case due to flexible nature of the
5 framework even at room temperature, CO₂ adsorption decreases at higher temperature
6 because of contraction in the framework. Recently selective uptake of CO₂ has been done by
7 a number of different groups wherein MOF featuring free N and carboxylate O atoms.³³⁻³⁵
8
9
10
11
12
13
14
15
16
17



18
19
20
21
22
23
24
25
26
27
28
29
30
31
32
33
34
35
36
37
38
39
40
41
42
43
44
45
46
47
48
49
50
51
52
53
54
55
56
57
58
59
60
Figure 2. Gas adsorption isotherm of **1**: CO₂ at 195 K temperature, H₂ and N₂ at 77 K temperature and 1 atm pressure.

This polymer shows different catalytic reactions without activating the framework due to the presence of free acidic groups (-COOH) inside the cavities which initiate the catalysis. On the other hand free C=O and N atoms of the benzimidazole groups are also present in the structure leading to the enhancement of the rate of the reaction. A great effect of the flexibility or breathing effect of the **1** even at room temperature which arises due to the presence of two large linkers having a number of free groups (non-coordinated) which can be adjusted according to the coordination mode of the metal ion. There are a number of metal

1
2
3 organic frameworks which undergo these type of reactions having Lewis acidic sites along
4 with the basic sites in the framework performing synergistic catalysis.³⁶⁻⁵³ Unsaturated metal
5 sites can be generated after removal of coordinated solvent molecules during activation at
6 high temperature. It takes a long time to prepare catalysts for the reaction. Recent MOFs
7 containing open metal sites along with MNPs (metal nanoparticles) embedded in the cavities
8 of the polymer have been synthesized for catalytic reactions.⁵⁴⁻⁶¹ In this case first MOF will
9 be synthesized after that NPs encapsulation occurs. It is not only a costly process but also a
10 time consuming process because activation is required after each cycle of the catalysis. In the
11 case of zeolites, size of the product molecule is limited by the size of the pore apertures as
12 well as these zeolitic structures are deactivated by the small amount of coke which can block
13 the access of the reactants towards the active sites.^{62, 63}

14
15 While molecular sieves are not only very expensive but also should not be exposed to water
16 due to giving off heat. Its dust can also irritate sensitive tissues as well as after following a
17 shutdown, temperatures in a molecular sieve bed can stay hot for weeks so bed should be
18 cooled properly to switch it for adsorption.

19 **Cycloaddition of CO₂ to Epoxides**

20
21 The structural observation of **1**, shows several important features like the presence of free
22 protonated carboxylic acid groups, carbonyl groups and the presence of Lewis basic sites
23 originating from the rich N-containing TBIB ligand. Because of the permanent porosity of the
24 framework with open channels it captures CO₂ selectively which enable substrate diffusion.
25 Due to these prominent features in **1**, heterogeneous catalytic activity has been evaluated
26 through the cycloaddition of CO₂ to various epoxides to yield value added product, cyclic
27 organic carbonates. Cyclic carbonates have gained much attention due to their broad
28 spectrum of applications such as polar aprotic solvents, electrolytes for lithium-ion batteries,
29 pharmaceutical/fine chemical intermediates, and in many biomedical applications.^{21,22} Cyclic
30
31
32
33
34
35
36
37
38
39
40
41
42
43
44
45
46
47
48
49
50
51
52
53
54
55
56
57
58
59
60

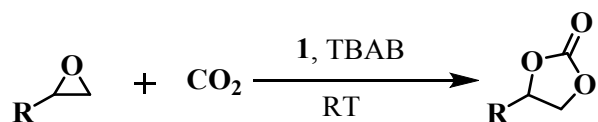
1
2
3 carbonates are also used as constituents of oils and paints and as monomers for the synthesis
4 of polycarbonates²³ and polyurethanes²² since they can undergo ring-opening polymerization.
5
6 The cycloaddition of styrene oxide with CO₂ into phenyl ethylene carbonate was selected as a
7
8 model reaction to explore the catalytic behaviour of the MOF. The cycloaddition reaction has
9
10 been carried out at room temperature, 1 atm pressure of CO₂ under solvent-free conditions
11
12 using catalyst (**1**, 30 mg) with tetra-*n*-tertbutylammonium bromide (TBAB, 60 mg) as co-
13
14 catalyst for 24 h. The results are summarized in Table 1. The cycloaddition reaction could not
15
16 occur remarkably in the absence of either of the MOF catalyst or co-catalyst (entry 5 and 6).
17
18 If H₃TCPB is taken as a homogeneous catalyst along with TBAB as a co-catalyst then 20%
19
20 yield of the cyclic carbonate is obtained. It was found that the styrene oxide could be
21
22 converted into the corresponding cyclic carbonate with excellent yield (>99 %) when both
23
24 catalyst and TBAB were used combinedly (entry 1).
25
26
27
28
29

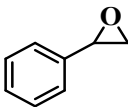
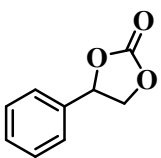
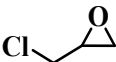
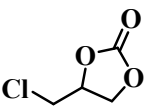
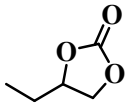
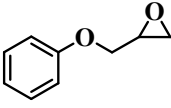
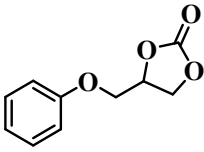
30
31 The activity of the catalyst was then evaluated in more depth. Such, high catalytic activity
32
33 was also observed for the cycloaddition of CO₂ with various epoxide substrates to produce
34
35 corresponding cyclic organic carbonates under the same reaction conditions (Table 1).
36
37 Specifically, epichlorohydrin and 1,2-butylene oxide reacts efficiently with the yields of
38
39 >99% (Table 1, entry 2) and >99% (Table 1, entry 3), respectively. Phenyl glycidyl ether was
40
41 little bit less reactive due to the steric effect of the substrates, while a yield of 82% was still
42
43 achieved (Table 1, entry 4).
44
45

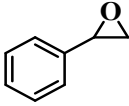
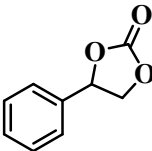
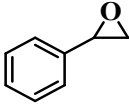
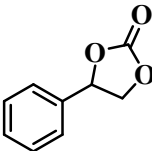
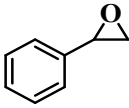
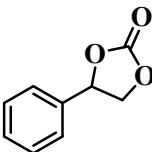
46
47 To judge the heterogeneous nature of the MOF catalyst, filtration test have been performed
48
49 with the model reaction using optimized reaction conditions to ensure that the catalytic
50
51 activities do not originate from leaching of any metal ions from the MOF structure. After 24
52
53 h, the MOF catalyst was removed by filtration and the reaction was allowed to continue. As
54
55 expected, there was no significant increase in the formation of styrene carbonate detected
56
57 after the MOF catalyst was removed. Indeed, this result primarily provides strong support for
58
59
60

the fact that the catalytic reaction was heterogeneous in nature. Recycling studies were then undertaken using the optimized conditions where the reaction mixture was filtered to collect the catalyst and washed several times with chloroform and then by acetone. After drying at room temperature the catalyst was regenerated and further used it for subsequent runs and checked its recyclability. In the model reaction, MOF catalyst was reused up to five successive times with the yield of styrene carbonate slightly decreasing in the first run to 82% after that yield is constant till fifth run (Figure S7). PXRD analysis was performed on the recycled MOF catalyst, in which structural preservation was proven (Figures S8).

Table 1. Coupling of various epoxides with CO₂ at room temperature and at atmospheric pressure using 1^a



Entry	Epoxide	Catalyst	Co-catalyst	Time (h)	Cyclic Carbonate	Yield (%) ^b
1		1	TBAB	24		>99
2		1	TBAB	24		>99
3		1	TBAB	24		>99
4		1	TBAB	24		82

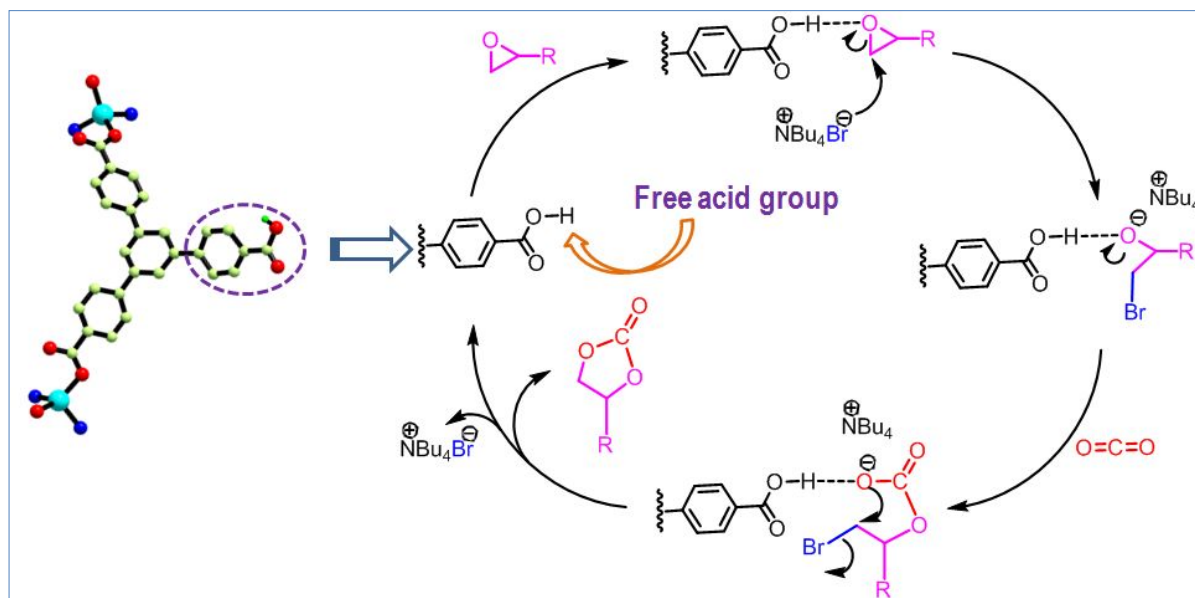
5		1	None	24		7
6		None	TBAB	24		12
7		H ₃ TCPB	TBAB	24		20

^aReactions were carried out in a 10 mL two-necked round bottom flask at room temperature and CO₂ bubbling. Epoxide (20 mmol, 1 equiv), **1** (0.0025 equiv), TBAB (0.05 equiv). No solvent was added.
^bYields were calculated using ¹H NMR analysis by integration of epoxide versus cyclic carbonate peaks (see the Supporting Information Figures S9-S12).

As heterogeneous catalyst **1** has free COOH, C=O groups (one COOH group and two C=O groups free for one H₃TCPB linker) along with non-coordinated benzimidazole N atoms which are decorated at the surface of the pores so there is no need to activate this catalyst due to the presence of protonated carboxylic acid groups. Recently cyclic carbonate formation in MOF was demonstrated by Li et al and Wang et al due to the presence of Lewis acidic metal sites and uncoordinated carboxylate O atoms.^{34, 35} Previous literature propose the mechanism that free carboxylic acid groups help in catalyzing the reaction efficiently.^{64,65} But framework was activated at higher temperature to remove lattice solvent molecules as well as coordinated solvent molecules. But in this case as-synthesized compound was used directly. COOH group of the catalyst initiates formation of non-covalent interaction with the epoxide substrate followed by ring opening through simultaneous nucleophilic attack of bromide ion from co-catalyst TBAB. After that CO₂ reacts with the O atom of the epoxide in a

electrophilic manner forming a carbonate intermediate. Finally cyclic carbonate is formed through intramolecular ring closure.

Scheme 1. Proposed mechanism for the synthesis of cyclic carbonate by the catalyst 1



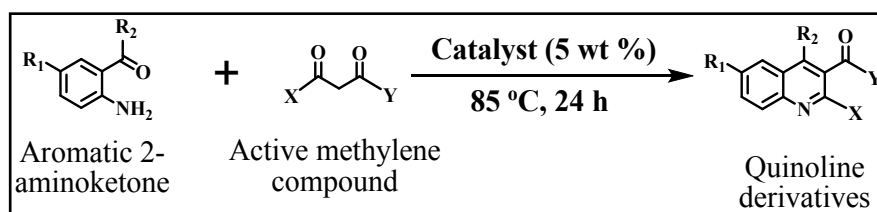
Friedländer reaction : synthesis of quinoline derivatives. As mentioned earlier that high thermal stability, large pore volume as well as free carboxylic acid (-COOH) groups along with the free C=O and -N, groups in the frameworks makes it a good Lewis acid heterogeneous catalyst. To check its Lewis acid nature, Lewis acid catalysed reaction has been performed. Here, synthesis of quinoline derivatives via the Friedländer reaction, has been demonstrated by employing catalyst **1** (Scheme 2). Quinoline is an important and ubiquitous backbone in innumerable biological and pharmaceutical molecules.⁶⁶ Quinoline derivatives exhibit antibacterial, antimalarial, anti-inflammatory, anti-asthmatic, anti-hypertensive and tyrosine kinase PDGF-RTK inhibiting properties.^{67, 68} Moreover, quinolines act as synthons for the synthesis of nanostructures and polymeric materials that convey the optoelectronic or NLO properties with excellent mechanical strengths.^{69, 70} Since, quinolines are important in industry, pharmacology and synthetic points of view, numerous versatile synthetic procedures have been reported for their synthesis.⁷¹⁻⁷⁴ Among those, the Friedländer

hetero-annulation is one of the most simple and a direct route for the quinoline synthesis. In Friedländer hetero-annulation reaction, different poly substituted quinoline derivatives have been synthesized through reaction between an aromatic 2-aminoaldehyde or ketone and an active methylene containing carbonyl compounds.^{75, 76} However, there has been tremendous development towards the synthesis of quinoline derivatives using acid catalyst, by avoiding the use of the traditionally basic conditions.⁷⁷⁻⁷⁹ Apart from conventional protic acids, many other catalysts have also been used for the Friedländer synthesis.^{80, 81} MOFs having open metal sites which act as Lewis-acids, have already shown catalytic activity for the Friedländer reaction.⁸² Perez-Mayoral et al. investigated CuBTC catalyzed Friedländer condensation by a combination of different experimental techniques as well as by DFT based modelling and found that CuBTC showed improved catalytic activity when compared with other MOFs e.g. in BEA and (Al)SBA-15 containing high concentration of Lewis acid sites.^{83, 84}

As already mentioned that the activation process to generate active sites or vacant metal sites is a prolonged process and the chances for the degradation of frameworks are increases.

In the present study, a carboxylate based Zn-MOF (**1**) has been designed that have free carboxylic acid groups at the pore surface of the framework. Catalytic behaviour of **1** showed its huge potential as a promising acidic heterogeneous catalyst for the synthesis of quinoline derivatives (Scheme 3).

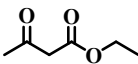
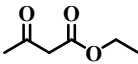
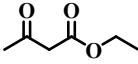
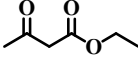
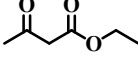
Scheme 2. Synthesis of quinoline derivatives via the Friedländer reaction between aromatic 2-aminoketone and active methylene compounds

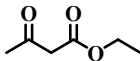
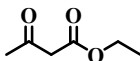


At first, the model reaction between 2-aminobenzophenone (0.5 mmol) and ethyl acetoacetate (1 mmol) have been done in the presence of **1** (5 wt%) at 85 °C for 24 h which gave the

desired compound in 97% isolated yield (Table 1, Entry 1). A possible mechanism for the synthesis of quinolines using this catalyst is shown in Scheme 3, where the free carboxylic acid group catalyses the reaction in the same way as shown by the vacant metal sites in CuBTC MOF due to the hard Lewis acid character.⁸³ It is shown in the Table 1 that the various aromatic 2-aminoketone (0.5 mmol) have been used with ethyl acetoacetate (1 mmol) in presence of catalyst **1** (5 wt%) under solvent-free conditions at 85 °C for 24 h, to give the respective quinoline derivatives in moderate to excellent yields. The 98% and 94% yields was observed with 4-chloro and 4-nitro substituted 2-aminobenzophenone respectively (Table 1, entries 2 and 3). Also, the catalytic activity of **1** was tested with 2-aminoacetophenone and ethyl acetoacetate (1 mmol) that afforded product with 95% Yield (Table 1, entry 4). The heterogeneous catalytic activity of **1** showed superiority over both the homogeneous zinc salt i.e. zinc acetate as well as the H₃TCPB which gave the desired product in low yields that is 26% and 21%, respectively (Table 1, entry 5 and 6). Also, the non-catalyst experiment was performed, in which 2-aminobenzophenone and ethyl acetoacetate was reacted in absence of any catalyst that showed very low yield (9%) (Table 2, entry 7), confirming the catalytic activity of **1**.

Table 2. Friedländer reaction between different aromatic 2-aminoketone and different active methylene compounds^[A]

Entry	Catalyst	Aromatic 2-aminoketone		Active methylene compound	Yield (%) ^[B]
		R ₁	R ₂		
1	1	H	Ph		97
2	1	Cl	Ph		98
3	1	NO ₂	Ph		94
4	1	H	Me		95
5	Zn(OAc) ₂ ·(H ₂ O) ₂	H	Ph		26

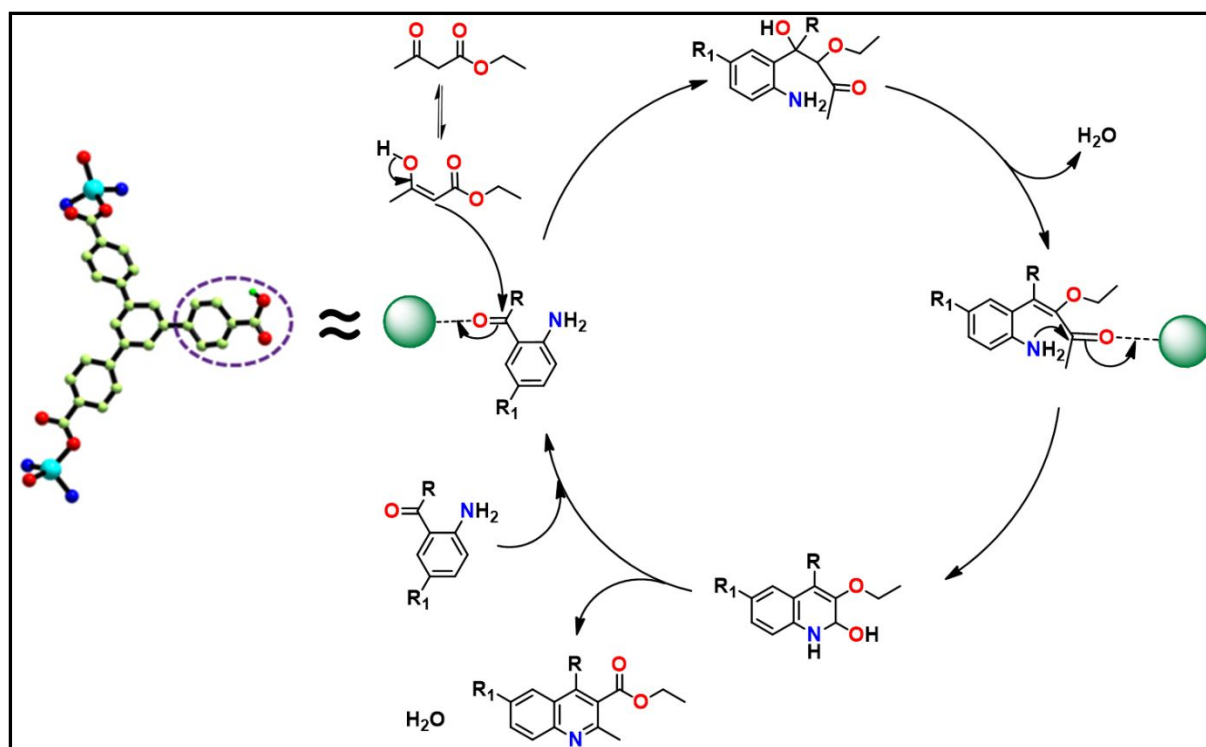
6	H₃TCPB	H	Ph		21
7	No Catalyst	H	Ph		9

[^A] 2-aminoaryl ketones (0.5 mmol), ethyl acetoacetate (1 mmol), and catalyst **1** (5 wt %), sealed tube 85 °C for 24 h. [^B] Yield of the isolated product after flash chromatography.

As described above, the heterogeneous nature of **1** was confirmed by the hot filtration experiment, as well as the framework is reusable and the framework integrity was maintained during the recyclability experiments.

These data show that **1** is a proficient Lewis-acid catalyst in Friedländer reactions with varied substrates. In each case, the characterization of desired product was achieved by the ¹H, ¹³C NMR spectroscopy (Figures S13–S20).

Scheme 3. Proposed Mechanism for the synthesis of quinoline derivatives through Friedländer reaction



CONCLUSIONS

Hydrothermally synthesized flexible Zn-based 2D porous coordination polymer shows selective CO₂ gas adsorption. It breathes at room temperature due to the presence of two large

1
2
3 size linkers, but at higher temperature flexibility is increased. It acts as an excellent
4 heterogeneous catalyst towards the chemical fixation of CO₂ to cyclic carbonates as well as
5
6 towards the synthesis of quinoline derivatives through Friedländer reaction. Catalytic activity
7
8 is due to the presence of free protonated COOH groups in the polymer which are decorated at
9
10 the surface of the pores. There are free C=O groups along with non-coordinated
11
12 benzimidazole N atoms which assist the reactivity of the catalyst.
13
14
15
16
17
18

19 ASSOCIATED CONTENT

21 Supporting Information

22
23 The Supporting Information is available free of charge on the ACS Publications website at
24
25 DOI ;
26
27

28 with Physical measurements, X-ray structural studies, IR, TGA, PXRD and NMR spectra.

29
30 X-ray crystallographic data of **1** (CCDC number -1819056).
31
32

33 AUTHOR INFORMATION

35 Corresponding Author

36
37 E-mail: rashmi.a.agarwal@gmail.com
38
39

40 Notes

41
42 The authors declare no competing financial interest.
43
44

45 ACKNOWLEDGMENTS

46
47 The authors would like to thank IIT Kanpur for extending facilities to undertake this study.
48
49
50

51 REFERENCES

- 52
53
54 1. O’Keeffe, M. Design of MOFs and intellectual content in reticular chemistry: a
55 personal view. *Chem. Soc. Rev.* **2009**, *38*, 1215–1217.
56
57
58 2. James, S. L. Metal-organic frameworks. *Chem. Soc. Rev.* **2003**, *32*, 276–288.
59
60

- 1
2
3 3. Champness, N. R. Coordination frameworks—where next? *Dalton Trans.* **2006**, *0*,
4 877–880.
5
6
- 7
8 4. Janiak, C. Functional Organic Analogues of Zeolites Based on Metal–Organic
9 Coordination Frameworks. *Angew. Chem., Int. Ed. Engl.* **1997**, *36*, 1431–1434.
10
11
- 12 5. Mueller, U.; Schubert, M.; Teich, F.; Puetter, H.; Schierle-Arndt, K.; Pastre', J.
13 Metal–organic frameworks—prospective industrial applications. *J. Mater. Chem.*
14 **2006**, *16*, 626–636;
15
16
17
- 18 6. Czaja, A. U.; Trukhan, N.; Muller, U. *Chem. Soc. Rev.* **2009**, *38*, 1284–1293.
19
20
- 21 7. Ferey, G. Some suggested perspectives for multifunctional hybrid porous solids.
22 *Dalton Trans.* **2009**, 4400–4415.
23
24
- 25 8. Tranchemontagne, D. J.; Zheng, N.; O'Keeffe, M.; Yaghi, O. M. *Angew. Chem. Int.*
26 *Ed.* **2008**, *47*, 5136–5147.
27
28
29
- 30 9. Allen, A. E.; MacMillan, D. W. C. *Chem. Sci.* **2012**, *3*, 633–658.
31
32
- 33 10. Li, X.-Y.; Li, Z.-J.; Li, Y.-Z.; Hou, L.; Zhu, Z.; Wang, Y.-Y. Direct Evidence:
34 Enhanced C₂H₆ and C₂H₄ Adsorption and Separation Performances by Introducing
35 Open Nitrogen-Donor Sites in a MOF *Inorg. Chem.* **2018**, *57*, 12417–12423.
36
37
38
- 39 11. Kitagawa, S.; Uemura, K. Dynamic porous properties of coordination polymers
40 inspired by hydrogen bonds. *Chem. Soc. Rev.* **2005**, *34*, 109–119.
41
42
43
- 44 12. Bureekaew, S.; Shimomura, S.; Kitagawa, S. Chemistry and application of flexible
45 porous coordination polymers. *Sci. Technol. Adv. Mater.* **2008**, *9*, 014108–014120.
46
47
48
- 49 13. Liu, Q.; Wu, L.; Jackstell, R.; Beller, M. Using Carbon Dioxide as a Building Block
50 in Organic Synthesis. *Nat. Commun.* **2015**, *6*, 5933–5948.
51
52
53
- 54 14. Trickett, C. A.; Helal, A.; Al-Maythaly, B. A.; Yamani, Z. H.; Cordova, K. E.;
55 Yaghi, O. M. The Chemistry of Metal–Organic Frameworks for CO₂ Capture,
56 Regeneration and Conversion. *Nat. Rev. Mater.* **2017**, *2*, 17045–17061.
57
58
59
60

- 1
2
3 15. Quadrelli, R.; Peterson, S. The energy-climate challenge: Recent trends in CO₂
4 emissions from fuel combustion *Energy Policy*, **2007**, *35*, 5938–5952.
5
6
7
8 16. Gupta, M.; De, D.; Tomar, K.; Bharadwaj, P. K. From Zn(II)-Carboxylate to Double-
9 Walled Zn(II)-Carboxylate Phosphate MOF: Change in the Framework Topology,
10 Capture and Conversion of CO₂, and Catalysis of Strecker Reaction. *Inorg. Chem.*
11 **2017**, *56*, 14605–14611.
12
13
14
15
16
17 17. Lee, H. M.; Youn, S.; Saleh, M.; Lee, J. W.; Kim, K. S. Interactions of CO₂ with
18 various functional molecules. *Phys. Chem. Chem. Phys.* **2015**, *17*, 10925–10933.
19
20
21
22 18. Pal, T. K.; De, D.; Neogi, S.; Pachfule, P.; Senthilkumar, S.; Xu, Q.; Bharadwaj P. K.
23 Significant Gas Adsorption and Catalytic Performance by a Robust CuII–MOF
24 Derived through Single-Crystal to Single-Crystal Transmetalation of a Thermally
25 Less-Stable ZnII–MOF. *Chem. Eur.J.* **2015**, *21*, 19064.
26
27
28
29
30
31 19. Zheng, B. S.; Bai, J. F.; Duan, J. G.; Wojtas, L.; Zaworotko, M. J. Enhanced CO₂
32 Binding Affinity of a High-Uptake rht-Type Metal–Organic Framework Decorated
33 with Acylamide Groups. *J. Am. Chem. Soc.* **2011**, *133*, 748–751.
34
35
36
37
38 20. Lehn, J.-M. *Supramolecular Chemistry: Concepts and Perspectives*. **1995**.
39
40 21. Agarwal, R. A. Structural Diversity and Luminescence Properties of Novel
41 $\{[\text{Cd}_3(\text{TBIB})_4(\text{BTC})_2] \cdot 2\text{C}_2\text{H}_5\text{OH} \cdot 11\text{H}_2\text{O}\}_n$ and $\{[\text{Zn}(\text{TBIB})(\text{HBTC})] \cdot 3\text{H}_2\text{O}\}_n$
42 Coordination polymers. *Polyhedron* **2015**, *85*, 740–747.
43
44
45
46
47 22. Kim, J.; Chen, B.; Reineke, T. M.; Li, H.; Eddaoudi, M.; Moler, D. B.; O’Keeffe, M.;
48 Yaghi, O. M. *J. Am. Chem. Soc.* **2001**, *123*, 8239–8247.
49
50
51
52 23. Harlick, P. J.-E., Sayari, A. Application of pore-expanded mesoporous silica 5.
53 Triamine grafted material with exceptional CO₂ dynamic and equilibrium adsorption
54 performance. *Ind. Eng. Chem. Res.* **2007**, *46*, 446–458.
55
56
57
58
59
60

- 1
2
3
4
5
6
7
8
9
10
11
12
13
14
15
16
17
18
19
20
21
22
23
24
25
26
27
28
29
30
31
32
33
34
35
36
37
38
39
40
41
42
43
44
45
46
47
48
49
50
51
52
53
54
55
56
57
58
59
60
24. Belmabkhout, Y.; Sayari, A. Effect of pore expansion and amine functionalization of mesoporous silica on CO₂ adsorption over a wide range of conditions. *Adsorption*, **2009**, *15*, 318–328.
25. Heydari-Gorji, A.; Yang, Y.; Sayari, A. Effect of the Pore Length on CO₂ Adsorption over Amine-Modified Mesoporous Silicas. *Energy Fuels*. **2011**, *25*, 4206–4210.
26. Zupal, A.; Arean, C. O.; Delgado, M. R.; Nachtigall, P.; Pulido, A.; Mayerová, J.; Cejka, J.; Combined volumetric, infrared spectroscopic and theoretical investigation of CO₂ adsorption on Na-A zeolite, *Microporous and Mesoporous Materials*. **2011**, *146*, 97–105.
27. Caskey, S. R.; Wong-Foy, A. G.; Matzger, A. J. Dramatic Tuning of Carbon Dioxide Uptake via Metal Substitution in a Coordination Polymer with Cylindrical Pores. *J. Am. Chem. Soc.* **2008**, *130*, 10870–10871.
28. Mason, J. A.; Sumida, K.; Herm, Z. R.; Krishna, R.; Long, J. R. Evaluating metal–organic frameworks for post-combustion carbon dioxide capture via temperature swing adsorption. *Energy Environ. Sci.* **2011**, *4*, 3030–3040.
29. Bao, Z.; Yu, L.; Ren, Q.; Lu, X.; Deng, S. Adsorption of CO₂ and CH₄ on a magnesium-based metal organic framework. *J. Colloid Interface Sci.* **2011**, *353*, 549–556.
30. Grajciar, L.; Wiersum, A. D.; Llewellyn, P. L.; Chang, J.-S.; Nachtigall, P. Understanding CO₂ Adsorption in CuBTC MOF: Comparing Combined DFT-Ab Initio Calculations with Microcalorimetry Experiments. *J. Phys. Chem. C*. **2011**, *115*, 17925–17933.
31. Liao, P.-Q.; Chen, X.-W.; Liu, S.-Y.; Li, X.-Y.; Xu, Y.-T.; Tang, M.; Rui, Z.; Ji, H.; Zhang, J.-P.; Chen, X.-M. Putting an ultrahigh concentration of amine groups into a

- 1
2
3 metal–organic framework for CO₂ capture at low pressures. *Chem. Sci.* **2016**, *7*, 6528–
4
5 6533.
6
7
8 32. Liao, P.-Q.; Chen, H.; Zhou, D.-D.; Liu, S.-Y.; He, C.-T.; Rui, Z.; Ji, H.; Zhang, J.-P.;
9
10 Chen, X.-M. Monodentate hydroxide as a super strong yet reversible active site for
11
12 CO₂ capture from high-humidity flue gas, *Energy Environ. Sci.* **2015**, *8*, 1011–1016.
13
14
15 33. Yang, H.-Y.; Li, Y.-Z.; Jiang, C.-Y.; Wang, H.-H.; Hou, L.; Wang, Y.-Y.; Zhu, Z. An
16
17 Interpenetrated Pillar-Layered Metal-Organic Framework with Novel Clusters:
18
19 Reversible Structural Transformation and Selective Gate-Opening Adsorption *Cryst.*
20
21 *Growth Des.* **2018**, *18*, 3044–3050.
22
23
24 34. Li, X.-Y.; Li, Y.-Z.; Yang, Y.; Hou, L.; Wang, Y.-Y.; Zhu, Z. Efficient light
25
26 hydrocarbon separation and CO₂ capture and conversion in a stable MOF with
27
28 oxalamide-decorated polar tubes† *Chem. Commun.* **2017**, *53*, 12970–12973.
29
30
31 35. Wang, H.-H.; Hou, L.; Li, Y.-Z.; Jiang, C.-Y.; Wang, Y.-Y.; Zhu, Z. Porous MOF
32
33 with Highly Efficient Selectivity and Chemical Conversion for CO₂. *ACS Appl. Mater.*
34
35 *Interfaces* **2017**, *9*, 17969–17976.
36
37
38 36. Aguirre-Diaz, L. M.; Gandara, F.; Iglesias, M.; Snejko, N.; Gutierrez-Puebla E.;
39
40 Monge, M. A'. Tunable Catalytic Activity of Solid Solution Metal–Organic
41
42 Frameworks in One-Pot Multicomponent Reactions. *J. Am. Chem. Soc.* **2015**, *137*,
43
44 6132–6135.
45
46
47 37. Mitchell, L.; Williamson, P.; Ehrlichov, B.; Anderson, A. E.; Seymour, V. R.;
48
49 Ashbrook, S. E.; Acerbi, N.; Daniels, L. M.; Walton, R. I.; Clarke, M. L.; Wright, P.
50
51 A. Mixed-metal MIL-100(Sc,M) (M=Al, Cr, Fe) for Lewis acid catalysis and tandem
52
53 C-C bond formation and alcohol oxidation. *Chem.–Eur. J.* **2014**, *20*, 17185–17197.
54
55
56 38. Schejn, A.; Aboulaich, A.; Balan, L.; Falk, V.; Laleve'e, J.; Medjahdi, G.; Aranda, L.;
57
58 Mozet, K.; Schneider, R. Cu²⁺-doped zeolitic imidazolate frameworks (ZIF-8):
59
60

- 1
2
3 efficient and stable catalysts for cycloadditions and condensation reactions. *Catal. Sci.*
4
5 *Technol.* **2015**, *5*, 1829–1839.
- 6
7
8 39. Lee, Y.-R.; Chung, Y.-M.; Ahn, W.-S. A new site-isolated acid–base bifunctional
9
10 metal–organic framework for one-pot tandem reaction. *RSC Adv.* **2014**, *4*, 23064–
11
12 23067.
- 13
14
15 40. Li, B.; Zhang, Y.; Ma, D.; Li, L.; Li, G.; Li, G.; Shi, Z.; Feng, S. A strategy toward
16
17 constructing a bifunctionalized MOF catalyst: post-synthetic modification of MOFs
18
19 on organic ligands and coordinatively unsaturated metal sites. *Chem. Commun.* **2012**,
20
21 *48*, 6151–6153.
- 22
23
24 41. Srirambalaji, R.; Hong, S.; Natarajan, R.; Yoon, M.; Hota, R.; Kim, Y.; Ko, Y. H.;
25
26 Kim, K. Tandem catalysis with a bifunctional site-isolated Lewis acid–Brønsted base
27
28 metal–organic framework, NH₂-MIL-101(Al). *Chem. Commun.* **2012**, *48*, 11650–
29
30 11652.
- 31
32
33 42. Toyao, T.; Fujiwaki, M.; Horiuchi, Y.; Matsuoka, M. Application of an amino-
34
35 functionalised metal–organic framework: an approach to a one-pot acid–base reaction.
36
37 *RSC Adv.* **2013**, *3*, 21582–21587.
- 38
39
40 43. Park, J.; Li, J. R.; Chen, Y. P.; Yu, J.; Yakovenko, A. A.; Wang, Z. U.; Sun, L. B.;
41
42 Balbuena, P. B.; Zhou, H. C. P. B.; Zhou, H. C. A versatile metal–organic framework
43
44 for carbon dioxide capture and cooperative catalysis. *Chem. Commun.* **2012**, *48*,
45
46 9995–9997.
- 47
48
49 44. Chizallet, C.; Lazare, S.; Bazer-Bachi, D.; Bonnier, F.; Lecocq, V.; Soyer, E.;
50
51 Quoineaud, A.-A.; Bats, N.; Catalysis of Transesterification by a Nonfunctionalized
52
53 Metal–Organic Framework: Acido-Basicity at the External Surface of ZIF-8 Probed
54
55 by FTIR and ab Initio Calculations. *J. Am. Chem. Soc.* **2010**, *132*, 12365–12377.
- 56
57
58
59
60

- 1
2
3 45. Zhang, F.; Wei, Y.; Wu, X.; Jiang, H.; Wang, W.; Li, H. Hollow Zeolitic Imidazolate
4 Framework Nanospheres as Highly Efficient Cooperative Catalysts for [3+3]
5 Cycloaddition Reactions. *J. Am. Chem. Soc.* **2014**, *136*, 13963–13966.
6
7
8
9
10 46. Kim, J.; Kim, S.-N.; Jang, H.-G.; Seo, G.; Ahn, W.-S. CO₂ cycloaddition of styrene
11 oxide over MOF catalysts. *Appl. Catal. A*, **2013**, *453*, 175–180.
12
13
14 47. Valvekens, P.; Vandichel, M.; Waroquier, M.; Van Speybroeck, V.; De Vos, D.
15 Metal-dioxidoterephthalate MOFs of the MOF-74 type: Microporous basic catalysts
16 with well-defined active sites. *J. Catal.* **2014**, *317*, 1–10.
17
18
19
20 48. Wu, P.; Wang, J.; Li, Y.; He, C.; Xie, Z.; Duan, C.; Luminescent Sensing and
21 Catalytic Performances of a Multifunctional Lanthanide-Organic Framework
22 Comprising a Triphenylamine Moiety. *Adv. Funct. Mater.* **2011**, *21*, 2788–2794.
23
24
25
26
27 49. Llabrés i Xamena, F. X.; Cirujano, F. G.; Corma, A. An unexpected bifunctional acid
28 base catalysis in IRMOF-3 for Knoevenagel condensation reactions. *Microporous*
29 *Mesoporous Mater.* **2012**, *157*, 112–117.
30
31
32
33
34 50. J. Gascon, U. Aktay, M. Hernandezalonso, G. Vanklink and F. Kapteijn, Amino-
35 based metal-organic frameworks as stable, highly active basic catalysts. *J. Catal.*
36 **2009**, *261*, 75–87.
37
38
39
40
41 51. A. M. Rasero-Almansa, A. Corma, M. Iglesias and F. Sánchez, Design of a
42 Bifunctional Ir–Zr Based Metal–Organic Framework Heterogeneous Catalyst for the
43 N-Alkylation of Amines with Alcohols. *ChemCatChem.* **2014**, *6*, 1794–1800.
44
45
46
47
48 52. Yang, Y.; Yao, H.-F.; Xi, F.-G.; Gao, E.-Q. Amino-functionalized Zr(IV) metal–
49 organic framework as bifunctional acid–base catalyst for Knoevenagel condensation.
50 *Mol. Catal. A: Chem.* **2014**, *390*, 198–205.
51
52
53
54
55
56
57
58
59
60

- 1
2
3 53. Vermoortele, F.; Ameloot, R.; Vimont, A.; Serre, C.; Vos, D. D. An amino-modified
4 Zr-terephthalate metal–organic framework as an acid–base catalyst for cross-aldol
5 condensation. *Chem. Commun.* **2011**, *47*, 1521–1523.
6
7
8
9
10 54. Pan, Y.; Yuan, B.; Li, Y.; He, D. Multifunctional catalysis by Pd@MIL-101: one-step
11 synthesis of methyl isobutyl ketone over palladium nanoparticles deposited on a
12 metal–organic framework. *Chem. Commun.* **2010**, *46*, 2280–2282.
13
14
15
16
17 55. Liu, H.; Li, Y.; Luque, R.; Jiang, H. A Tuneable Bifunctional Water-Compatible
18 Heterogeneous Catalyst for the Selective Aqueous Hydrogenation of Phenols. *Adv.*
19 *Synth. Catal.* **2011**, *353*, 3107–3113.
20
21
22
23
24 56. Ertas, I. E.; Gulcan, M.; Bulut, A.; Yurderi, M.; Zahmakiran, M. Rhodium
25 nanoparticles stabilized by sulfonic acid functionalized metal-organic framework for
26 the selective hydrogenation of phenol to cyclohexanone. *J. Mol. Catal. A: Chem.*
27 **2015**, *410*, 209–220.
28
29
30
31
32
33 57. Cirujano, F. G.; Llabrés i Xamena, F. X.; Corma, A. MOFs as multifunctional
34 catalysts: One-pot synthesis of menthol from citronellal over a bifunctional MIL-101
35 catalyst. *Dalton Trans.* **2012**, *41*, 4249–4254.
36
37
38
39
40 58. Cirujano, F. G.; Leyva-Perez, A.; Corma, A.; Llabrés i Xamena F. X. MOFs as
41 Multifunctional Catalysts: Synthesis of Secondary Arylamines, Quinolines, Pyrroles,
42 and Arylpyrrolidines over Bifunctional MIL-101. *ChemCatChem.* **2013**, *5*, 538–549.
43
44
45
46
47 59. Chen, Y.-Z.; Zhou, Y.-X.; Wang, H.; Lu, J.; Uchida, T.; Xu, Q.; Yu, S.-H.; Jiang, H.-
48 L. Multifunctional PdAg@MIL-101 for One-Pot Cascade Reactions: Combination of
49 Host–Guest Cooperation and Bimetallic Synergy in Catalysis. *ACS Catal.* **2015**, *5*,
50 2062–2069.
51
52
53
54
55
56
57
58
59
60

- 1
2
3 60. Liu, H.; Li, Y.; Jiang, H.; Vargas, C.; Luque, R. Significant promoting effects of
4 Lewis acidity on Au–Pd systems in the selective oxidation of aromatic hydrocarbons.
5
6 *Chem. Commun.* **2012**, *48*, 8431–8433.
7
8
9
10 61. Li, X.; Guo, Z.; Xiao, C.; Goh, T. W.; Tesfagaber, D.; Huang, W. Tandem Catalysis
11 by Palladium Nanoclusters Encapsulated in Metal–Organic Frameworks. *ACS Catal.*
12 **2014**, *4*, 3490–3497.
13
14
15
16 62. Guisnet, M.; Magnoux, P. Coking and Deactivation of Zeolites-Influence of the Pore
17 Structure. *Appl. Catal.* **1989**, *54*, 1–27.
18
19
20
21 63. Perot, G.; Guisnet, M. *J. Mol. Catal.* **1990**, *61*, 173–196.
22
23
24 64. Nguyen, P. T. K.; Nguyen, H. T. D.; Nguyen, H. N.; Trickett, C. A.; Ton, Q. T.;
25 Gutiérrez-Puebla, E.; Monge, M. A.; Cordova, K. E.; Gándara, F. New
26 Metal–Organic Frameworks for Chemical Fixation of CO₂. *ACS Appl. Mater.*
27 *Interfaces* **2018**, *10*, 733–744.
28
29
30
31 65. Li, Y.-Z.; Wang, H.-H.; Yang, H. Y.; Hou, L.; Wang, Y.-Y.; Zhu, Z. An Uncommon
32 Carboxyl-Decorated Metal–Organic Framework with Selective Gas Adsorption and
33 Catalytic Conversion of CO₂. *Chem. Eur. J.* **2018**, *24*, 865–871.
34
35
36
37 66. Chen, Y. L.; Fang, K. C.; Sheu, J. Y.; Hsu, S. L.; Tzeng, C. C. Synthesis and
38 antibacterial evaluation of certain quinolone derivatives. *J. Med. Chem.* **2001**, *44*,
39 2374–2377.
40
41
42
43 67. Roma, G.; Braccio, M. D.; Grossi, G.; Chia, M. 1,8-Naphthyridines IV. 9-Substituted
44 N,N-dialkyl-5-(alkylamino or cycloalkylamino) [1,2,4]triazolo[4,3-
45 a][1,8]naphthyridine-6-carboxamides, new compounds with anti-aggressive and
46 potent anti-inflammatory activities. *Eur. J. Med. Chem.* **2000**, *35*, 1021–1035.
47
48
49
50
51
52
53
54
55
56
57
58
59
60

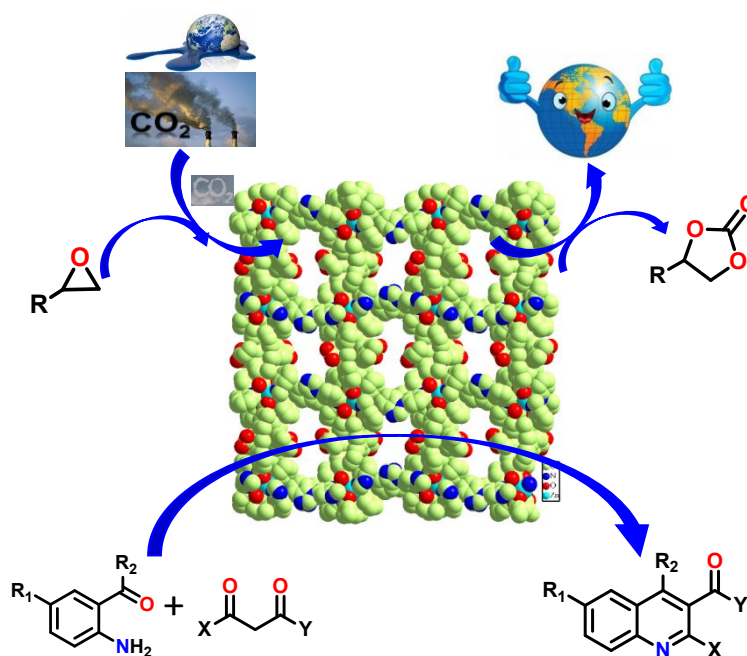
- 1
2
3
4
5
6
7
8
9
10
11
12
13
14
15
16
17
18
19
20
21
22
23
24
25
26
27
28
29
30
31
32
33
34
35
36
37
38
39
40
41
42
43
44
45
46
47
48
49
50
51
52
53
54
55
56
57
58
59
60
68. Bilker, O.; Lindo, V.; Panico, M.; Etiene, A. E.; Paxton, T.; Dell, A.; Rogers, M.; Sinden, R. E.; Morris, H. R. Identification of xanthurenic acid as the putative inducer of malaria development in the mosquito. *Nature* **1998**, *392*, 289–292.
69. Zhang, X.; Jenekhe, S. A. Electroluminescence of Multicomponent Conjugated Polymers. 1. Roles of Polymer/Polymer Interfaces in Emission Enhancement and Voltage-Tunable Multicolor Emission in Semiconducting Polymer/Polymer Heterojunctions. *Macromolecules* **2000**, *33*, 2069–2082.
70. Jenekhe, S. A.; Lu, L.; Alam, M. M. New Conjugated Polymers with Donor–Acceptor Architectures: Synthesis and Photophysics of Carbazole–Quinoline and Phenothiazine–Quinoline Copolymers and Oligomers Exhibiting Large Intramolecular Charge Transfer. *Macromolecules* **2001**, *34*, 7315–7324.
71. Kouznetsov, V. V.; M'endez, L. Y. V.; Gómez, C. M. M. Recent progress in the synthesis of quinolones. *Curr. Org. Chem.* **2005**, *9*, 141–161.
72. Jones, G. in *Comprehensive Heterocyclic Chemistry II*, eds. Katritzky, A. R.; Rees, C. W.; Scriven, E. F. V. Pergamon, New York, **1996**, *5*, 167.
73. Jiang, B.; Si, Y.-G. Zn(II)-Mediated Alkynylation–Cyclization of o-Trifluoroacetyl Anilines: One-Pot Synthesis of 4-Trifluoromethyl-Substituted Quinoline Derivatives. *J. Org. Chem.* **2002**, *67*, 9449–9451.
74. Linderman, R. J.; Kirolos, K. S. Regioselective synthesis of trifluoromethyl substituted quinolines from trifluoroacetyl acetylenes. *Tetrahedron Lett.* **1990**, *31*, 2689–2692.
75. Friedlaender, P. About o-amidobenzaldehyde. *Reports of the German Chemical Society* **1882**, *15*, 2572.
76. Cheng, C.-C.; Yan, S.-J. The Friedländer Synthesis of Quinolines. *Org. React.* **1982**, *28*, 37.

- 1
2
3 77. Sabitha, G.; Babu, R. S.; Subba Reddy, B. V.; Yadav, J. S. Microwave Assisted
4
5 Friedländer Condensation Catalyzed by Clay. *Synth. Commun.* **1999**, *29*, 4403–4408.
6
7
8 78. Wu, J.; Xia, H.-G.; Gao, K. Molecular iodine: a highly efficient catalyst in the
9
10 synthesis of quinolines via Friedländer annulation. *Org. Biomol. Chem* **2006**, *4*,
11
12 126–129.
13
14
15 79. Niknam, K.; Zolfigol, M. A.; Dehghani, A. Friedlander quinoline synthesis catalyzed
16
17 by $M(\text{HSO}_4)_n$ ($M = \text{Al, Mg, Ca}$) under solvent-free conditions. *Heterocycles* **2008**, *75*,
18
19 2513–2521.
20
21
22 80. Ghassamipour, S.; Sardarian, A. R. Friedländer synthesis of poly-substituted
23
24 quinolines in the presence of dodecylphosphonic acid (DPA) as a highly efficient,
25
26 recyclable and novel catalyst in aqueous media and solvent-free conditions.
27
28 *Tetrahedron Lett.* **2009**, *50*, 514–519.
29
30
31 81. Marco-Contelles, J.; Pérez-Mayoral, E.; Samadi, A.; do Carmo Carreiras, M.; Soriano,
32
33 E. Recent Advances in the Friedländer Reaction. *Chem. Rev.* **2009**, *109*, 2652–2671.
34
35
36 82. Gupta, A. K.; De, D.; Bharadwaj, P. K. A NbO type Cu(II) metal–organic framework
37
38 showing efficient catalytic activity in the Friedländer and Henry reactions. *Dalton*
39
40 *Trans.* **2017**, *46*, 7782–7790.
41
42
43 83. Pérez-Mayoral, E.; Musilová, Z.; Gil, B.; Marszalek, B.; Položij, M.; Nachtigall, P.;
44
45 Čejka, J. Synthesis of quinolines via Friedländer reaction catalyzed by CuBTC metal–
46
47 organic-framework. *Dalton Trans.* **2012**, *41*, 4036–4044.
48
49
50 84. Pérez-Mayoral, E.; Čejka, J. $[\text{Cu}_3(\text{BTC})_2]$: A Metal–Organic Framework Catalyst for
51
52 the Friedländer Reaction. *ChemCatChem.* **2011**, *3*, 157–159.
53
54
55
56
57
58
59
60

For Table of Contents Use Only

Flexible Zn-MOF Exhibiting Selective CO₂ Adsorption and Efficient Lewis Acidic Catalytic Activity

Rashmi A. Agarwal,^{a*} Anoop K. Gupta,^b Dinesh De^b



Zn(II) based flexible porous coordination polymer shows excellent heterogeneous catalytic activity due to the presence of Lewis acidic groups in the large linkers. Transformation of CO₂ into cyclic carbonates as well as synthesis of quinoline derivatives through Friedländer reaction could be done successfully by using this polymer.